Atomization Characteristics in Pneumatic Counterflowing Internal Mixing Nozzle

Sam Goo Lee
Graduate School, Department of Precision Mechanical Engineering, Chonbuk National University
Byung Joon Rho*
Faculty of Mechanical Engineering., Chonbuk National University and Automobile High Technology Research Institute

In an effort to illustrate the global variation of SMD (Sauter mean diameter, or D_{32}) and AMD (Arithmetic mean diameter, or D_{10}) at five axial downstream locations (i. e., at Z=30, 50, 80, 120, and 170 mm) under the different experimental conditions, the radial coordinate is normalized by the spray half-width. Experimental data to analyze the atomization characteristics concerning with an internal mixing type have been obtained using a PDPA (Phase Doppler Particle Analyzer). The air injection pressure was varied from 40 kPa to 120 kPa. In this study, counterflowing internal mixing nozzles manufactured at an angle of 15°with axi-symmetric tangential-drilled four holes have been considered. By comparing the results, it is clearly possible to discern the effects of increasing air pressure, suggesting that the disintegration process is enhanced and finer spray droplets can be obtained under higher air assist. The variations in D_{32} are attributed to the characteristic feature of internal mixing nozzle in which the droplets are preferentially ejected downward with strong axial momentum, and dispersed with the larger droplets which are detected in the spray centerline at the near stations and smaller ones are generated due to further subsequent breakup by higher shear stresses at farther axial locations. The poor atomization around the centre close to the nozzle exit is attributed to the fact that the relatively lower rates of spherical particles are detected and these drops are not subject to instantaneous breakup in spite of the strong axial momentum. However, substantial increases in SMD from the central part toward the edge of the spray as they go farther downstream are mainly due to the fact that the relative velocity of droplet is too low to cause any subsequent disintegration.

Key Words : SMD, AMD, PDPA, Counterflowing Internal nozzle

1. Introduction

In many calculations of mass transfer and flow processes it is convenient to work only with mean or average diameters instead of the complete drop size distribution. The concept of the mean diameter has been generalized by Mugele and Evans (1951). The most common diameters are SMD and AMD for combustion analysis and spray flow. AMD is the linear average value of all the drops in spray; and SMD is the diameter of the drop whose ratio of volume to surface area is the same as that of entire spray.

Spray combustion is widely employed in many industrial energy conversion processes including the industrial furnaces and boilers, liquid rocket combustion systems, gas turbines, internal combustion engines and other liquid-fuel fired sys-

* Corresponding Author,
E-mail : sglee@moak.Chonbuk.ac.kr
TEL : +82-63-270-2370 ; **FAX** : +82-63-277-7308
Faculty of Mechanical Engineering., Chonbuk National University and Automobile High Technology Research Institute, 664-14, Duckjin-dong, Duckjin-gu, Chonju, Chonbuk 561-756, Korea. (Manuscript **Received** September 27, 1999 ; **Revised** July 7, 2000)

tems. Many attempts have been carried out for the spray behavior with interferometric techniques like PDPA, which measured the droplet velocity and size simultaneously for droplets passing through the measurement volume of two laser beams.

The purpose of breaking up the liquid into multitudinous droplets is to increase the liquid surface area and achieve high relative velocity for atomization to get the heat and mass transfer improvement. The function of atomizer is not only to disintegrate the liquid into small droplets but also to discharge into the ambient gaseous medium with a symmetrical uniform and fine spray. Research works for the twin-fluid atomizers have been carried out, but the studies on the disintegration mechanism are still being investigated to characterize the optimum models. In order to promote an mixing formation between two working fluids, qualitative consistency of atomization through much better air/liquid mixing is required. Atomization of a liquid using twin fluid atomizers is most effectively achieved by generating a high relative velocity between a liquid jet and the surrounding gas. Several parameters are known to play a significant role in controlling the dynamics of the mixing processes; air/liquid mass flow rate ratio, aerodynamic effects by the surrounding air flow pattern and nozzle geometric configuration. Regarding the aerodynamic consideration, one of the top prerequisites for good atomization is getting a high momentum of the droplets, that is, the appropriate rapid velocity and high turbulence intensity caused by interactions between working fluids.

A large number of publications in this field have been described on the disintegration process issuing from the twin-fluid atomizer. Rho, et al. (1995) derived an expression for a correlation between SMD and Presser et al. (1996) reported that the distributions of droplet trajectory angle are wider under swirling conditions. Mullinger et al. (1974) concluded that the internal mixing atomizers gain an advantage over the external mixing type. Eroglu et al. (1991) showed that the relative velocity at the liquid/air interface increased with air supply pressure. Mao (1987) also reported that the SMD and ALR had a linear correlation, Lefebvre (1992) studied the factors influencing mean drop size. Elkotp et al. (1978) analyzed the atomization performance in the geometrically swirling atomizer. Rosa et al. (1989) reported the effect of swirl using a PDPA. Rao and Lefebvre (1975) have shown that an increase in fuel injection pressure and air velocity tend to produce better atomization. Rho et al. (1998) investigated on the swirl characteristics, and concluded that the air velocity and optimum swirl were the most important factors influencing droplet atomization.

The aim in this experimental investigation is to describe atomization phenomena in a spray issuing from an internal mixing counterflowing axisymmetric jets. The liquid is inflowed through the tangential ports that give the liquid and air an angular velocity and interacted together in the mixing chamber and dispersed into the stagnant ambient air. To characterize the global features of the spray, atomization characteristics such as the droplet diameter, volume flux, number density, and spray trajectory angle are measured using a 3-D PDPA.

2. Experimental Apparatus and Method

The prototype nozzle for generating a counterflowing spray is fabricated of brass. The nozzle configuration used to establish counter-flowing mixing in an axisymmetric jet is schematically shown in Fig. 1. The discharge orifice diameter d_o is 2 mm, swirl chamber diameter (D_s) is 9 mm, the length/diameter ratio of the discharge orifice is 0.65 ($l_o \fallingdotseq 1.3$), and 15° of counter-swirl to the central axis has been utilized.

The experimental apparatus used to measure the spray characteristics is shown schematically in Fig. 2. Continuous and steady atomizing water and the pulsation-free air are supplied to the mixing chamber from the pressurized storage tank compressed by air. Compressed air and water are properly filtered and regulated. A number of valves, pressure gauges, and flow meters are located in the nozzle feed line to provide the desired operating conditions. Experiments were conduct-

ed for the liquid flow rate, $\dot{m}_l$, was kept constant value at 7.95 g/s and the air pressures were gradually increased from 20 kPa to 200 kPa, namely, air flow rate, $\dot{m}_a$, was increased stepwise as $\dot{m}_a/\dot{m}_l=0.054-0.132$ by adjusting the valves. Three representative air pressures are chosen (P_a =0.4, 0.8 and 1.2 bar) in this paper. Since the liquid velocity is maintained constant, an increase in air velocity (namely, increase of air-pressure) leads to an increase in air-liquid relative velocity or air density in the spray field, consequently imposing higher aerodynamic force on the liquid. Working fluid and pressurized air by a compressor are fed into a swirl chamber through the respective tangentially drilled inlets (d_w and d_a= 1.5mm) that give the liquid and air a high angular velocity, thereby creating an interaction within the swirl chamber and dispersing into the quiescent ambient air. Coordinate Z corresponds to the streamwise droplets moving in the downstream direction at the nozzle exit and y signifies the radially outward motion. The radial quantities are normalized by the half-value width of the velocity distribution. The half-velocity width is the distance from the axis of a point where the mean streamwise velocity is half its value on the streamwise axis. The measurement volume can be positioned easily at various stations without moving the diagnostic systems in three orthogonal

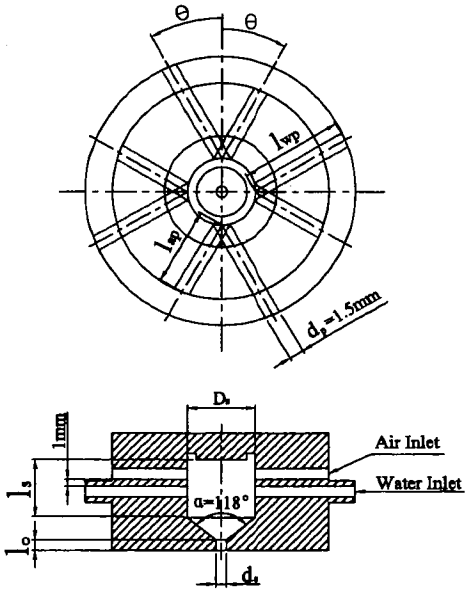

Fig. 1 Schematic configuration of internal mixing counterflowing atomizer

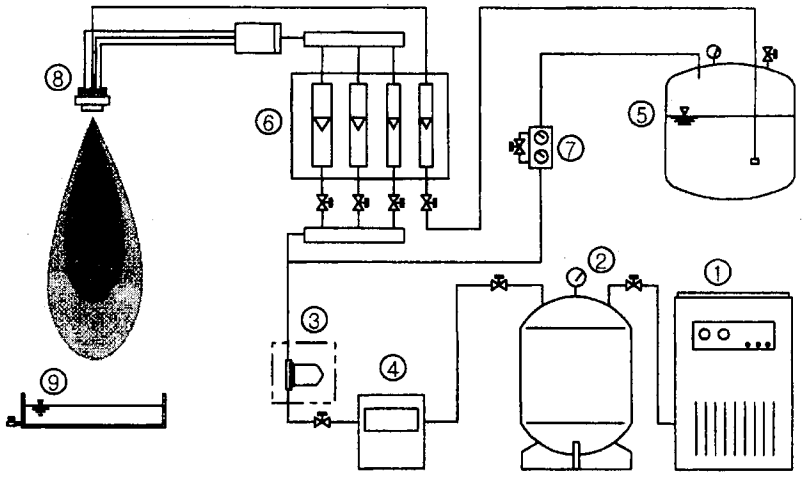

Fig. 2 Schematic diagram for the air and liquid supply systems

directions by using a computer controlled traversing system that permits positioning to within 0.01 mm.

A PDPA is installed to specify spray flows, which have been conducted along the axial downstream distances from the nozzle exit. The PDPA provides the information on individual particle size between 1 μm and 250 μm passing through the measurement volume in this investigation. The focal lengths of the transmitting and receiving optics were 400 mm and 500 mm, respectively. The photomuitiplier detector voltage of 1400 V was optimized to provide the maximum sensitivity, and 45° of scattering was made in the forward direction. A bragg cell was used to shift the frequency of one beam of each pair by 40 MHz to provide directional sensitivity and to prevent fringe bias.

The radial profiles of a geometric sequence space to quantify the spray trajectory at each measurement locations were obtained at 5 axial stations of Z=30, 50, 80, 120, and 170 mm downstream from the nozzle exit. The droplet quantities were calculated by collecting 10,000 samples at each point. The sampling time depended on the local number density of drops, and 10 seconds was set as an upper limit to record meaningful data. Every precaution was taken to avoid possible sources of error during the experiments such as power fluctuations, mistracking the particles, nozzle vibrations, temperature changes in the laboratory and the reading of flow meters, etc. Also, the mists of small droplets generated were collected in a collection tank to prevent splashing and then discharged to an exhaust system attached to the side of the collection tank. For repeatability of the experimental data, each profile was checked by measuring the data at least twice.

The ratio of signal to noise and data acceptance rate were too low for distances less than 20 mm from the nozzle exit. Reasons for the low S/N are usually attributed to the presence of nonspherical particles in the PDPA probe volume. Because the PDPA works on the principle of light scattering by spherical particles, signals from nonspherical particles would be rejected by the instrument. Data acceptance rate varied from 60 to 98 % depending on the experimental conditions and the location of the probe volume in relation to the spray geometry. Acceptance rates were the highest at low liquid injection rates and modest distances from the nozzle exit. The spray was checked for axial symmetry in a few selected cases across the entire spray, but no significant asymmetry was noticed.

3. Results and Discussion

3.1 Droplet mean diameter

Figure 3 shows the variation of the droplet mean diameters along the axial downstream. All of the five stations shown in Fig. 3 have the same trend that is quite symmetric about the center region and shows qualitative consistency in data scatter even with increasing distances. D_{10} has nearly the same distribution pattern like SMD profiles and decreases evidently at downstream in the spray center. It is quite interesting to consider that the droplets at upstream regions (i. e., Z=30 -50 mm) in the center part are typically larger than those off the axis. At Z =30 mm, D_{10} is maximum ($\fallingdotseq$50-70 μm) on the centerline (y/b= 0) and decreases to $\fallingdotseq$35-48 μm at the spray periphery (y/b > 2). D_{32} is larger (88-120 μm) because it reflects the volume and the surface area of the droplets, weighting more on larger drops.

As a breakup mechanism in the central region, an initial increase of SMD may be due to the possibility of droplet coalescence that exists between the smaller and larger droplets despite of strong axial momentum, showing that the SMD decreases from approximately 88-120 μm at Z= 30 mm to 63-73 μm at Z=170 mm in the spray centerline. Note also that the profile for the spray at Z=30-80 mm exhibits a minimum in the spray boundary. For example, it increases from 50-77μ m at Z=30 mm to 70-95 μm at Z=170 mm in the spray sheet region, namely, y/b>2.5. This is attributed to the fact that the droplets at upstream are presumably affected with the higher swirl components which are displacing the bulk of the droplets radially outward from the center region than those affected most by strong axial momen-

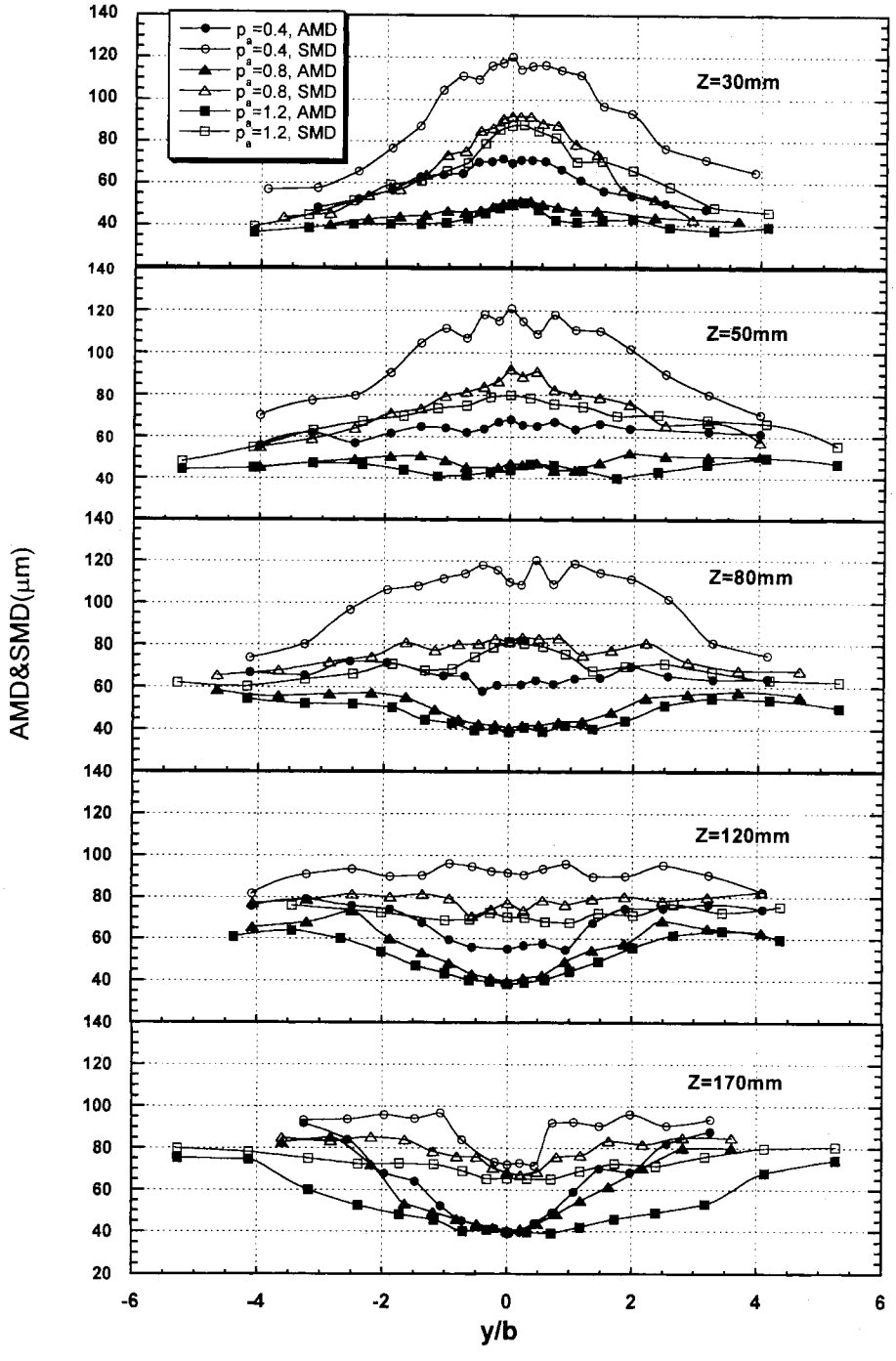

Fig. 3 Variation of SMD and AMD with radial position y/b measured at different axial positions Z

tum in the center region. As the spray spread out downstream (Z =80-170 mm), however, the maximum values of both D_{10} and D_{32} in spray periphery increase, which might be explained by the droplet transport (i. e., entrainment) from the outer part of the spray to the central region. This result is consistent with the previous observation by Takahashi et al. (1995) that the smaller dro-

plets in the peripheral region tend to be entrained inwardly and the larger droplets tend to remain in the region. Consequently, the smaller droplet mean diameters are less abundant in the centre region (see, Figs. 4-5) and the presence of relatively smaller ones near the spray boundary, which is valid only for the upstream locations (i. e., up to Z≒80 mm), is attributed to the breakup of the larger droplets that are caused by the characteristic feature of this internal mixing counter-flowing nozzles at the center. Since the larger droplets are dispersed faster than the smaller ones, the number of large droplets relative to small ones increases and causes an increase of the mean diameters up to the region of Z=50 mm, whereas the subsequent decrease from Z=80 mm can be seen due to secondary atomization. Thus, it can be explained that the fully developed atomization might be started from this axial location. This is diametrically opposite phenomena when compared to the previous investigations reported by Rho (1998) for two-phase flows, Dodge and Moses (1984) for a simplex pressure-atomizing nozzle, and by Yule et al. (1983) with a twin -fluid atomizer.

The SMD values decrease with an increase in air supply pressure, which provides higher relative velocity at the interface of the liquid and gas phases, and it is well established that SMD is inversely proportional to the relative velocity. Lorenzetto and Lefebvre (1977] also reached the same conclusion. The relative velocity required for disintegration could only be provided in this experiment as the air supply pressure is increased (40 kPa-120 kPa). At higher air supply pressures, the SMD values of the central peak seem to be more sensitive to the radial variation than those at lower air supply pressure. This result agrees with those of Mao et al. (1986, 1987), Presser et al. (1988, 1989), Mcdonell et al. (1992), and (1998).

Figure 4 exhibits the variation of SMD along the axial centerline downstream. It shows that an increase in p_a, which corresponds to an increase in atomizing air velocity, has a beneficial effect on atomization quality. Previous studies (1992) indicated that the Sauter Mean Diameter increases

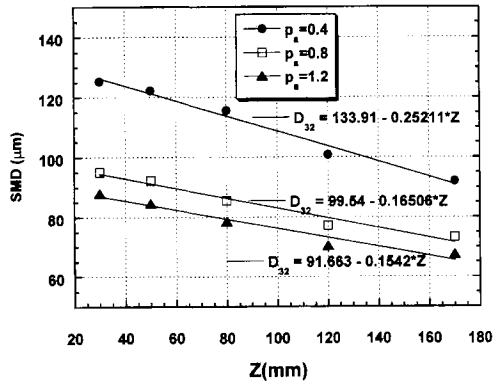

Fig. 4 Variation of SMD with axial positions measured along the centerline

with liquid flow rate. But, increasing the atomizing air pressure in the present experiments leads to an increased air/liquid flow ratio, which reduces the droplet size. This trend has been well proved in other studies. Figure 4 shows that the lower air injection pressure indicates steeper increase in D_{32} than for the higher case at all axial locations. The rate of decrease in SMD is greatly reduced at high air flow rates, and the strong linear correlation of SMD along the axial distances is maintained, but beyond a certain air flow rate, further increase does not produce brisk atomization. The symmetric profiles of SMD at y/b=0 along the axial locations demonstrate similar results investigated by Zhou et al. (1997). This correlation implies that the atomization in this nozzle has a strong dependence on the air supply pressure, which is similar to those obtained by Sankar et al. (1994) or by Eroglu and Chigier (1991). As the axial distance increased, the SMD decreased in the outer regions of spray, indicating that the smaller droplets were being entrained into the central region of spray. The SMD lies in the range of 40-120 μm for the cases tested in this study as discussed in other result by Issac (1994).

3.2 Volume flux

To understand why D_{32} is the highest in the center at upstream locations, Fig. 5 presents normalized droplet volume flux distributions from Z=30 to 120 mm axial stations. The peak in volume flux is coincident with the distribution in

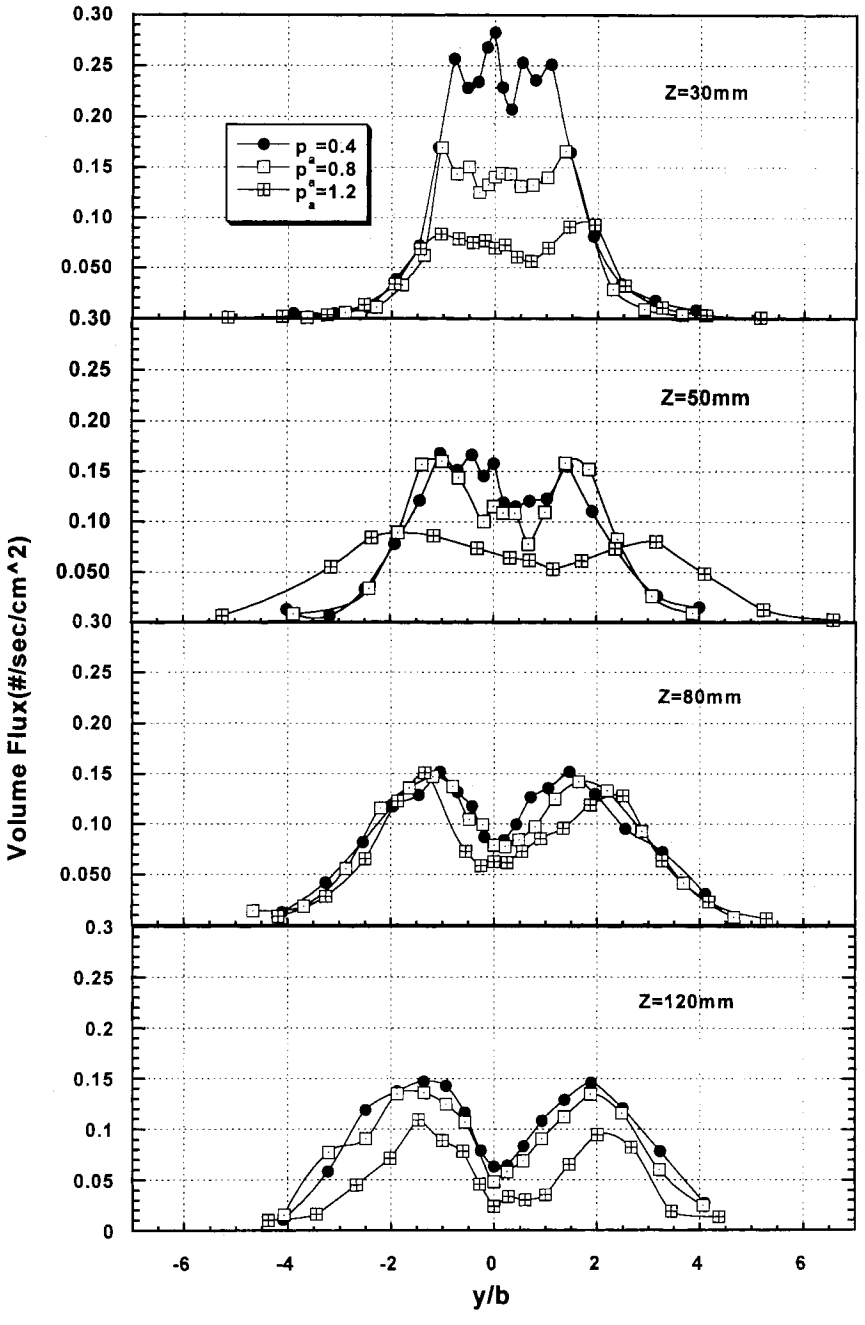

Fig. 5 Variation of volume flux with radial position y/b measured at different axial positions Z

D_{32} at upstream regions. The careful examination of these normalized profiles shows a discernible difference at Z=30 mm, and in the presence of higher air pressure, the volume fluxes are evidently reduced at all axial locations, which is the same trend with the SMD distribution as shown in Fig. 3. At Z=30 mm, the high rate of volume fluxes are existed on the axis, and it is nearly uniform pattern even in the radial boundary sprays, while being surrounded by droplets having a dilute concentration in the spray boundary. At Z=50 mm, there is a small transfer of drops both quanti-

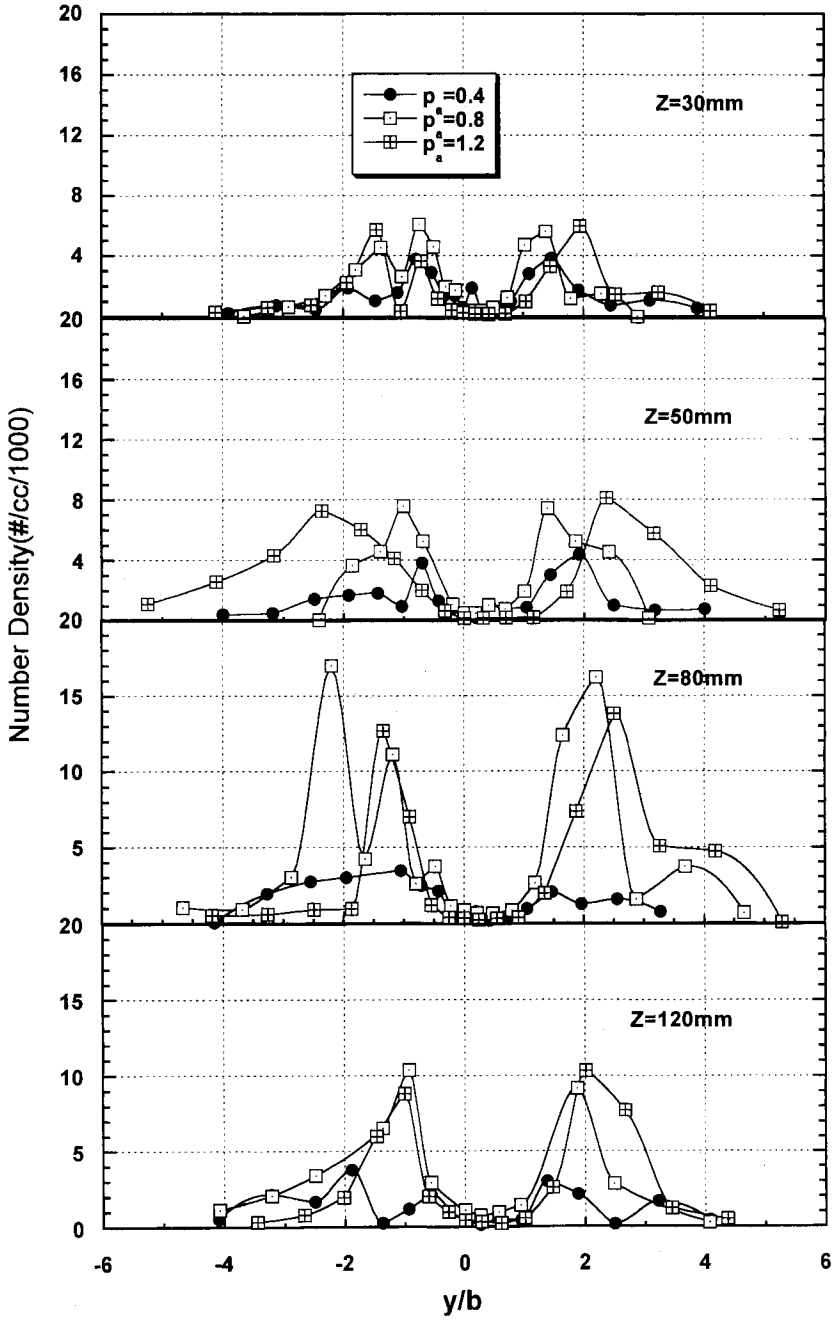

Fig. 6 Variation of number density with radial position y/b measured at different axial positions Z

tatively and qualitatively at the central region, although most of the comparative droplet concentration for the dense is intact because of the rapid spreading of the droplets in the process of disintegration. The highest volume flux at downstream $Z > 80$ mm is concentrated mainly near the spray periphery due to the comparative large size and the high number density (see, Fig. 6). It is coincident with the SMD profiles as discussed before. The volume fluxes at farther downstream decrease due to the less-abundant volume concentration for the larger droplets in the centre, suggesting

improved atomization. The reason for this is that the supply of atomizing air tends to reduce the volume flux across the cross-sectional area of spray. This is evidently substantiated by the fact that the distribution of the volume flux for the higher air-supply case is narrower and smaller than for the lower one, indicating a more positive influence on the spray volume flux under high air supply condition.

3.3 Number Density

In order to substantiate the global change of SMD, the distribution of number density in the spray field is necessary. The number density is the number of droplets per unit volume. Figure 6 represents the radial distributions of droplet number density. In the region near the nozzle exit, the droplet concentration for three cases remains essentially the same. The presence of two outer peaks due to the concentration of relatively larger droplets indicates that the positions of the spray boundary is coincident with volume flux distribution (see, Fig. 5). Number density reaches a maximum value of approximately N = 6000 droplets $/cm^3$ near the nozzle exit (i. e., at Z=30 mm), and increases to about N = 10000 - 15000 droplets $/cm^3$ at farther downstream.

The previous results obtained by Rho(1998) showed that the droplet number density for an external oriented swirling case decreased more rapidly due to the greater jet expansion and faster decay of droplet axial velocity. However, it is interesting to consider that the profiles for the number density in this experiment show no definite dissimilarity depending on the presence of higher air flow rates, resulting in a more uniform distribution of number density across the spray when compared. This is attributed to the comparative large axial momentum issuing from an internal mixing nozzle which leads consequently to longer strong penetration. Obviously, there should be a drop coalescence as a primary mechanism for this little change in number density. Two outward peaks in number density provide evidence of the significant increase of the larger drops in the spray periphery. Since the large drops have the higher inertia, they remain in the spray boundary and the small drops are easily transported to the central regions as discussed before. A similar result was reported by Lai et al. (1996). But the trend is not the same as those in the upper regions due to the prevailing concentration of the smaller droplets. Although the variations are smeared out, the particle number density for lower air supply appears to remain approximately the same. However, the local number density for higher air pressure increases monotonously with axial distance, indicating that relatively fewer particles have dispersed before Z < 50 mm. Thus, the higher air supply causes the particles to form clusters of high number density.

3.4 Spray angle

The entrainment of droplets by the surrounding gaseous medium and secondary breakup in spray is complicated. Using the droplet U and V velocity components information related to the droplet mean trajectory angle θ, which is defined as $\theta = 2\tan^{-1}(V/U)$, can be indirectly obtained. For the conditions of spray with swirl, the droplet tangential velocity component decays rapidly and becomes negligible. Variation of the droplet mean angle is presented in Fig. 7 at the various aforementioned locations. These data display special trends with regard to the effect of increasing injection pressure. It is quite interesting to note that the cone angle measurements have nearly the similar slope pattern, and that the cone angle data are not as widely dispersed as those obtained by the previous results obtained by Rho (1998).

The average cone angle near the spray periphery (i. e., y/b>3) for the higher air supply case is nearly 41.75°, whereas for the lower case is almost 50.75°. This corresponds to a 18 % decrease in cone angle as the relative injection velocity is raised. It should also be pointed out that the data do not appear to be approaching an asymptotic value in this pressure range. Thus, further increases in injection pressure would be expected to produce further narrowing of the cone angle. In the central regions (i. e., y/b<0.5) of spray, there is little difference in the direction of droplet motion between sprays at all axial downstream locations. That is, the spray cone angle is preser-

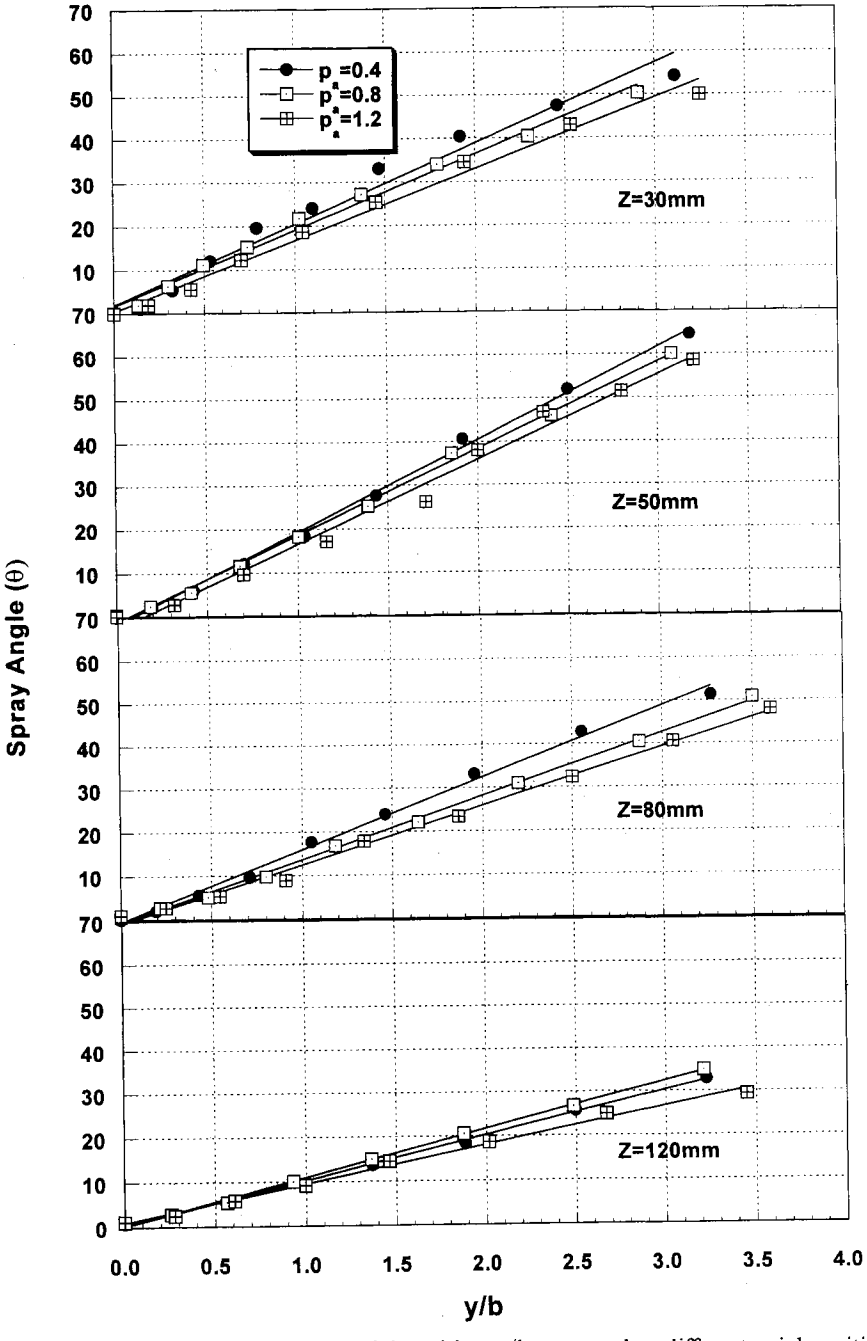

Fig. 7 Variation of spray angle with radial position y/b measured at different axial positions Z

ved, maintaining the droplet mean angle at approximately less than 10°. The range of spray angle was approximately 28°~62° based on the PDPA measurement. It might be inferred that the narrower spray angle was due to the rapid expansion accompanied with the higher air supply pressure.

4. Conclusion

The SMD shows higher values on the axis which are presumably attributed to the relatively

lower rates of spherical particles despite of their strong axial momentum at upstream regions. At farther downstream, however, the distributions of both D_{10} and D_{32} are inverted to the cases of upstream regions which might be explained by the droplet entrainment from the outer part of spray to the central region. The relative velocity increases with the air pressure due to the incresse of the air density. Hence, the higher the air injection pressure, the smaller the SMD. The decrease of drop size in the central downstream region implies a decrease in volume flux which is substantially in good agreement with the distribution of number density. So, it can be explained that the volume fluxes are proportional to the SMD variations. It shows a much clearer tendency of decreasing cone angle as the air supply pressure goes up. The reason for this is that the narrower spray angle is due to the rapid expansion accompanied with the higher air supply pressure. It turns out that the two outward peaks in number density is due mainly to the deflection of small drops as a primary mechanism that is responsible for. Because the large drops have the higher inertia, they remain in the spray boundary but the small drops are relatively easily transported to the central regions.

Reference

Beck, J. E., Lefebvre, A. H. and Koblish, T. R., 1991, "Liquid Sheet Disintegration by Impinging Air Streams," *Atomization and Sprays*, Vol. 1, pp. 155~170.

Brena de la Rosa, A., Bachalo, W. D., and Rudoff, R. C., 1989, " Spray Characterization and Turbulence Properties in an Isothermal Spray with Swirl," ASME paper No. 89-GT-273, *34th ASME International Gas Turbine & Aeroengine Congress*, Toronto, Canada, June.

Dodge, L. G., and Moses, C. A., 1984, *20th Symposium International on Combustion*, The Combustion Institute, Pittsburgh, p. 1239.

Elkotp, M. M., Rafat, N. M., and Hanna, M. A., 1978, "The Influence of Swirl Atomizer Geometry on the Atomization Performance," *ICLASS*, pp. 109~115.

Eroglu, H. and Chigier, N. A., 1991, "Initial Drop Size and Velocity Distributions for Airblast Coaxial Atomizers," *J. Fluids Eng.*, Vol. 113, pp. 453~459.

Issac, K., Missoum, A., Drallmeier, J. and Johnson, A., 1994, "Atomization Experiments in a Coaxial Coflowing Mach 1. 5 Flow," *AIAA Journal*, Vol. 32, No. 8, Aug.

Jean, J. Karl, Daniel Huilier, and Henri Burnage, 1996, "Mean Behavior of a Coaxial Air-Blast Atomized Spray in a Co-flowing Air Stream," *Atomization and Sprays*, Vol. 6, pp. 409~433.

Lai, W. H., Yang, K. H., Hong, C. H. and Wang, M. R., 1996, "Droplet Transport in Simplex and Air-Assisted Sprays," *Atomization and Sprays*, Vol. 6, pp. 27~49.

Lefebvre, A. H., 1992, "Twin-Fluid Atomization : Factors Influencing Mean Drop Size," *Atomization and sprays*, pp. 101~119.

Lorenzetto, G. E., and Lefebvre, A. H., 1977, " Measurements of Drop Size on a Plain Jet Airblast Atomizer," *AIAA Journall, Vol. 15, No. 7, pp. 1006~1010.*

Mao, C. P., 1987, "Drop size Distribution and Air Velocity Measurements in Air Assist Swirl Atomizer Sprays," *ASME*, Vol. 109, pp. 64~69.

Mao, C. P., Wang, G. and Chigier, N. 1986, "An Experimental Study of Air Assist Atomizer Spray Flames," 21st Symp. (Int.) on Combustion, pp. 665~673.

Mcdonell, V. G., Samuelsen, G. S., Wang, M. R., Hong, C. H. and Lai, W. H., 1992, "Interlaboratory Comparison of Phase Doppler Measurements in a Research Simplex Atomizer Sprays, AIAA Paper 92-3233, *AIAA/SAE/ASME/ASEE-20th* Joint Propulsion Conf. and Exhibit, Nashville, TN.

Mugele, R., and Evans, H. D., 1951, "Droplet Size Distribution in Sprays," *Ind. Eng. Chem.*, Vol. 43, No. 6, pp. 1317~1324.

Mullinger, P. J. and Chigier, N. A., 1974, "The Design and Performance of Internal Mixing Multijet Twin Fluid Atomizers," *J. of the Institute of Fuel, Dec.*, pp. 251~261.

Presser, C., Avedisian, C. T., Hodges. J. T. and Gupta, A. K., 1996, "Behavior of Droplets in

Pressure-Atomized Fuel Sprays with Coflowing Air Swirl," Progress in Astronautics and Aeronautics, Vol. 2, Chap. 2, pp. 31~62.

Rao, K. V. L. and Lefebvre, A. H., 1975, "Fuel Atomization in a Flowing Airstream," *AIAA Journal*, vol. 13, Oct. pp. 1413~1415.

Rho, B. J., Kang, S. J. and Oh, J. H., 1995, "An Experimental Study on the Atomization Characteristics of a Two-Phase Turbulent Jet of Liquid Sheet Type Co-Axial Nozzle," *Transactions of KSME*, vol 19, No. 6, pp. 1529~1538.

Rho, B. J., Lee, S. G. and Oh, J. H., 1998, "Swirl Effect on the Spray Characteristics of a Twin-Fluid Jet," *KSME International Journal*, Vol. 12, No. 5, pp. 899-906.

Rho, B. J., Lee, S. G., Kim, W. T. and Kang. S. J., 1998, "On the Intermittent Spray Characteristics," *KSME International Journal*, Vol. 12. No. 5, pp. 907~916.

Presser, C., Gupta, A. K. and Semerjian, H. G., 1988, "Aerodynamic Effects on Fuel Spray Characteristics; Air-Assist Atomizer," *ASME HTD*, Vol. 2, pp. 111~119.

Presser, C., Gupta, A. K. and Semerjian, H. G., 1989 "Droplet Velocity Measurements in a Swirling Kerosene Spray Flame," *ASME, HTD*-Vol. 122, pp. 21~34.

Sankar, S. V., Zhu, J. Y., and Bachalo, W. D., 1994, "Experimental Studies on the Behavior of Coaxial Injectors Using Liquid/Gaseous Nitrigen," *ICLASS* 94, pp. 672~679.

Takahashi, F. and Schmoll, W. J., 1995, "Characteristics of a Velocity Modulated Pressure Swirl Atomizing Spray," *J. of Propulsion and Power*, Vol. 11, No. 5, Sep. -Oct., pp. 955~962.

Yule, A. J., Ereaut, P. R., and Ungut, A., 1983, *Combustion Flame*, 54:15~22.

Zhou, Y., Lee, S., Robert L. Kozarek, and Enrique J. Lavernia, 1997, "Influence of Operating Variables on Average Droplet Size During Linear Atomization," *Atomization and Sprays*, Vol. 7, pp. 339~358.